11th International Conference
on Meson-Nucleon Physics and
the Structure of the Nucleon
September10-14, 2007
IKP, Forschungzentrum Jülich, Germany

HERMES Results on Hard-Exclusive Processes and Prospects Using the New Recoil Detector

Inti Lehmann, for the HERMES Collaboration
Department of Physics & Astronomy
University of Glasgow
Glasgow, G12 8QQ
Scotland, UK

Abstract

Hard exclusive processes provide access to the still unknown Generalised Parton Distributions (GPDs) which extend our description of the nucleon structure beyond the description by standard parton distributions. The HERMES experiment at DESY Hamburg studies hard exclusive processes using polarised electron or positron beams from HERA and an internal gas target.

Latest results are presented on Deeply Virtual Compton Scattering (DVCS) based on data taken with polarised hydrogen and deuterium targets, analysing events in the forward magnetic spectrometer. In particular the asymmetry measured on a transversely polarised proton target is sensitive to the GPD E; and it becomes possible to constrain the angular momentum fraction carried by u and d quarks.

Measuring the recoiling proton in addition to the forward scattered particles in those reactions reduces background and systematic uncertainties to a large extent. The newly built Recoil Detector was designed for this purpose. It was installed and commissioned at the beginning of 2006. First detector performance plots and an outlook of the physics topics addressed are given.

1 Physics Case

It has been known for decades that the nucleon can be described in all its quantum numbers by a combination of three quarks. However, it was then found that, in contrast to the naïve picture, the fraction of the spin 1/2 of the proton carried by the quarks is far below one. This caused considerable excitement when first observed. By now this fraction is well established to be about 1/3 [1]. The remainder must be somehow shared between a

contribution from the orbital angular momentum of the quarks and the total angular momentum of the gluons.

The structure of the nucleon as a system of quarks and gluons is traditionally described in terms of form factors and Parton Distribution Functions (PDFs). Elastic form factors describe the distribution of partons in impact parameter space while the PDFs describe their longitudinal momentum fraction. The theoretical framework of Generalised Parton Distributions (GPDs) [2–5] extends this to a more complete description of the nucleon. There are four main chirality conserving quark GPDs: $H_q(x,\xi,t)$, $E_q(x,\xi,t)$, $\widetilde{H}_q(x,\xi,t)$, $\widetilde{E}_q(x,\xi,t)$, where x, ξ, and t are the momentum fraction carried by the struck parton, the skewness, and the Mandelstam variable t, i.e. the squared momentum transfer to the target proton, respectively (refer to Fig. 1). In fact, the PDFs q and Δq are kinematic limits as $t \to 0$ of the GPDs H and $\widetilde{H}$ respectively. Elastic form factors of the nucleon can be obtained by calculating the first x moments of the four main GPDs.

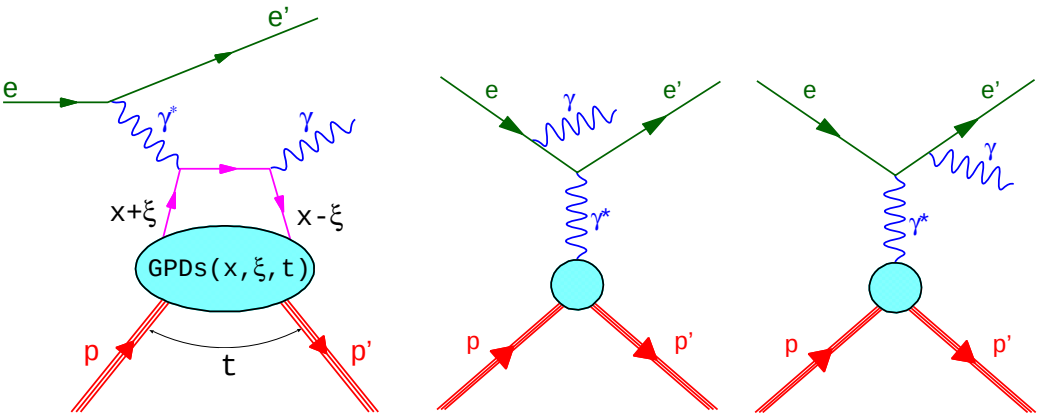

Figure 1: Left: Deeply Virtual Compton Scattering (DVCS). The incoming lepton emits a virtual photon, which scatters off a parton with momentum fraction $x + \xi$. This parton emits a real photon and returns to the nucleon with momentum fraction $x - \xi$. The momentum transfer between the initial and final nucleon state is $\sqrt{t}$. Right: the Bethe Heitler process (BH) is the dominant and indistinguishable experimental background which is, however, exactly calculable.

It has been noted that the total angular momentum of the quarks with flavour q is related to the GPDs H_q and E_q in the limit as $t \to 0$ (known as

the Ji Sum Rule [4]):

$$J_q = \lim_{t\to 0} \frac{1}{2} \int_{-1}^{+1} x\, dx [H_q(x,\xi,t) + E_q(x,\xi,t)]\,. \tag{1}$$

Hence measurements constraining these GPDs provide access to the angular momentum of the quarks.

Generalised Parton Distributions can be studied measuring Deeply Virtual Compton Scattering processes. DVCS processes involve a 'hard part' which can be described perturbatively and a 'soft part' which is described by GPDs. The hard part describes the scattering of the virtual photon off a parton with subsequent emission a hard real photon. In the soft part, GPDs describe the correlation between kinematic variables of the parton before interacting with the virtual photon and after emission of the real photon. (See Fig. 1.) This description is valid in the kinematical domain of large momentum transfer by the virtual photon Q^2 and small t.

The Bethe-Heitler (BH) process, i.e. the initial or final state radiation of a hard photon, leads to the same final state and cannot be distinguished by measurement at all. The total cross section measured experimentally is then given by

$$d\sigma(eN \to eN\gamma) \propto |T_{\mathrm{DVCS}}|^2 + |T_{\mathrm{BH}}|^2 + \underbrace{T_{\mathrm{DVCS}}\, T^*_{\mathrm{BH}} + T^*_{\mathrm{DVCS}}\, T_{\mathrm{BH}}}_{\mathrm{InterferenceTerm}}\,. \tag{2}$$

Although the BH amplitude T_{BH} is the dominant contribution in the kinematic conditions of the measurements, it is precisely calculable from measured elastic form factors of the nucleon. Thus one can extract the DVCS amplitude T_{DVCS} from a measurement of cross sections using the Interference Term of Eq. 2.

Experimentally these amplitudes can be accessed through the measurement of asymmetries. The four most important ones are: the Beam Spin Asymmetry (BSA)

$$A_{LU} = \frac{d\sigma(e^{\rightarrow},\phi) - d\sigma(e^{\leftarrow},\phi)}{d\sigma(e^{\rightarrow},\phi) + d\sigma(e^{\leftarrow},\phi)} \;\propto\; \Im m(\mathcal{H})\, \sin(\phi)\,, \tag{3}$$

the Beam Charge Asymmetry (BCA):

$$A_C = \frac{d\sigma(e^{+},\phi) - d\sigma(e^{-},\phi)}{d\sigma(e^{+},\phi) + d\sigma(e^{-},\phi)} \;\propto\; \Re e(\mathcal{H})\, \cos(\phi)\,, \tag{4}$$

the Longitudinal Target Spin Asymmetry:

$$A_{UL} = \frac{d\sigma(p^{\rightarrow},\phi) - d\sigma(p^{\leftarrow},\phi)}{d\sigma(p^{\rightarrow},\phi) + d\sigma(p^{\leftarrow},\phi)} \;\propto\; \Im m(\widetilde{\mathcal{H}})\, \sin(\phi)\,, \tag{5}$$

and the Transverse Target Spin Asymmetry:

$$\begin{aligned} A_{UT} = \frac{d\sigma(p^{\uparrow},\phi) - d\sigma(p^{\downarrow},\phi)}{d\sigma(p^{\uparrow},\phi) + d\sigma(p^{\downarrow},\phi)} \;\propto \\ \Im m(F_2\mathcal{H} - F_1\mathcal{E})\,\sin(\phi-\phi_S)\,\cos(\phi) \\ + \Im m(F_2\widetilde{\mathcal{H}} - F_1\xi\widetilde{\mathcal{E}})\,\cos(\phi-\phi_S)\,\sin(\phi)\,, \end{aligned} \tag{6}$$

where the arrows denote the polarisation of the beam electron e^- (positron e^+) or target proton p. These asymmetries are to leading order proportional to the real and imaginary parts of the Compton Form Factors (CFFs) $\mathcal{H}$, $\widetilde{\mathcal{H}}$, $\mathcal{E}$, $\widetilde{\mathcal{E}}$, and trigonometric functions of the angle ϕ between the lepton plane and the plane which is spanned by the virtual and real photons. F_1 and F_2 are the Dirac and Pauli Form Factors respectively. The Transverse Target Spin Asymmetry also depends on another azimuthal angle ϕ_S which relates the target spin vector to the lepton plane. At leading order in α_S the real and imaginary parts of the CFFs directly relate to the GPDs at $x = \pm\xi$ through:

$$\begin{aligned} \Im m\mathcal{F}(\xi,t) &= \pi\sum_q e_q^2\left[F_q(\xi,\xi,t) \mp F_q(-\xi,\xi,t)\right] \quad \text{and} \\ \Re e\mathcal{F}(\xi,t) &= -\sum_q e_q^2\left[P\int_{-1}^{+1} dx F_q(\xi,\xi,t)\left(\frac{1}{x-\xi} \mp \frac{1}{x+\xi}\right)\right], \end{aligned} \tag{7}$$

where the $\mathcal{F}(\xi,t)$ correspond to the CCFs $\mathcal{H},\mathcal{E}$ and $\widetilde{\mathcal{H}},\widetilde{\mathcal{E}}$ for (–) and (+) respectively [6]. Similarly, $F_q(x,\xi,t)$ are substitutes for the GPDs $H_q(x,\xi,t)$, $E_q(x,\xi,t)$, $\widetilde{H}_q(x,\xi,t)$, and $\widetilde{E}_q(x,\xi,t)$. P denotes Cauchy's principal value.

2 Results from HERMES

The HERMES experiment at DESY Hamburg [7] has been investigating the quark and gluon structure of the nucleon using electrons or positrons with 27.6 GeV energy from HERA scattered off protons or heavier nuclei. HERMES is an experiment consisting of a forward magnetic spectrometer and a storage cell target using gases ranging from Hydrogen to Krypton. Hydrogen and Deuterium targets can be polarised transversely or longitudinally.

The selection of the DVCS/BH process at HERMES requires events with exactly one photon and one charged track, identified as the scattered lepton, with $Q^2 > 1\,\mathrm{GeV}^2$. In the dataset where the recoiling proton has not been detected (before 2006), exclusive events are identified by requiring the missing mass M_X of the reaction $ep \to e\gamma X$ to correspond to the proton mass. Due

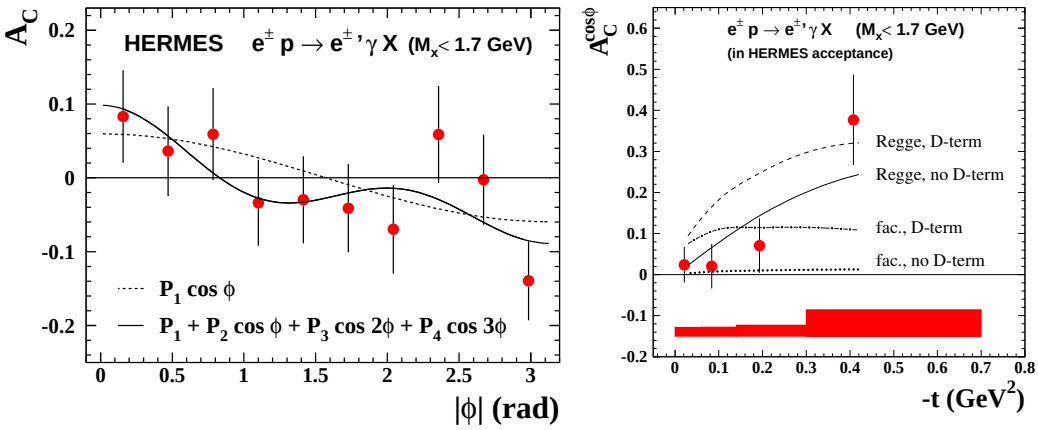

Figure 2: Left: Beam Charge Asymmetry A_C as a function of the azimuthal angle ϕ before background correction. The dashed curve shows the angular dependence extracted from the 4 parameter fit (solid line). Right: obtained $\cos\phi$ amplitude as a function of $-t$. These data restrict GPD models [10] shown as curves. Please refer to text and Ref. [11] for details.

to the finite energy resolution, the exclusive sample is selected in the region $-1.5 < M_X < 1.7\,\text{GeV}$, based on signal-to-background studies using Monte Carlo simulations.

HERMES and CLAS were the first experiments to measure the Beam-Spin Asymmetry A_{LU} in hard exclusive reactions [8, 9]. The Beam-Charge Asymmetry A_C has been measured on a proton target for the first time. The data disfavour a certain GPD model with the non-factorised t dependence (Regge) and including the D-term [10]. For details please refer to Fig. 2 and Ref. [11]. In Fig. 2 and the top panel of Fig. 3 the error bars and bands at the bottom of the panels represent the statistical and systematic uncertainties, respectively.

The Transverse Target Spin Asymmetry A_{UT} is the only asymmetry on a proton target where the contribution of the GPD E is not suppressed, i.e. the $\mathcal{H}$ term in Eq. 6 is smaller than the $\mathcal{E}$ term. The latter term is sensitive to the angular momentum of the quarks while the former is not [12]. The measured amplitude $A_{\text{UT}}^{\sin(\phi-\phi_S)\cos(\phi)}$ can be compared with a GPD model [13] varying the angular contribution of u and d quarks separately. An example of the variation of the u quark contribution is shown in the top panel of Fig. 3. In the bottom panel the resulting contour plot for an one-sigma band obtained from the data is shown. For further information please refer to Refs. [12, 14].

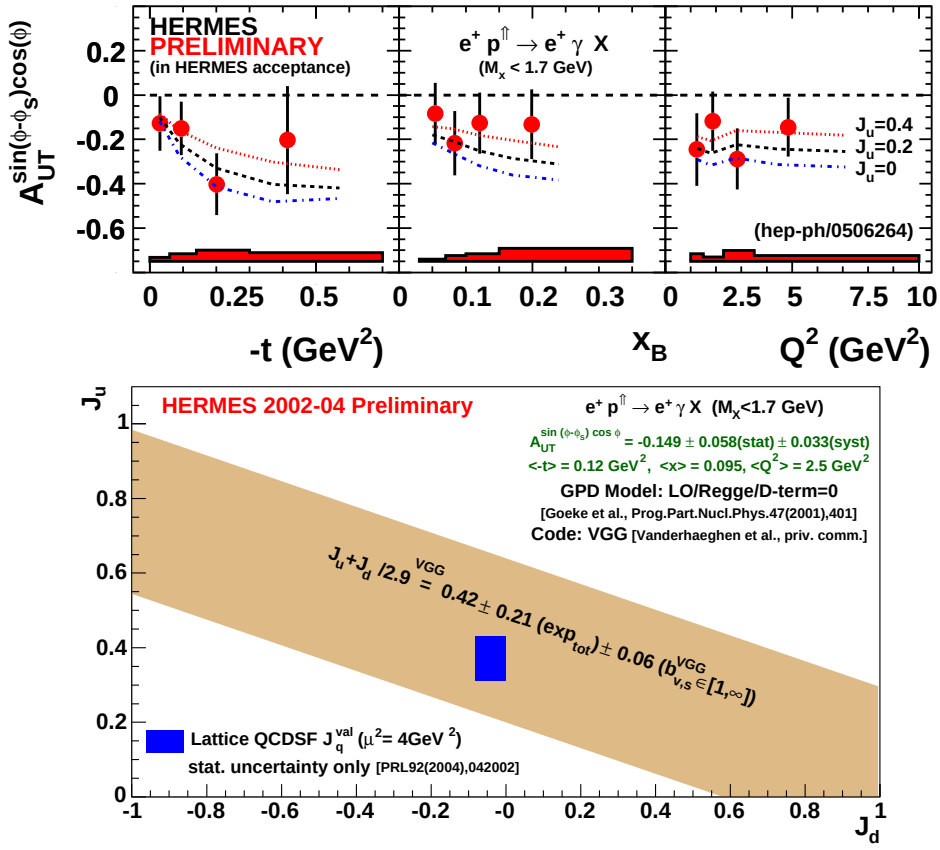

Figure 3: Top: the $A_{UT}^{\sin}(\phi-\phi_S)\cos\phi$ moment as a function of $-t, x_B$ or Q^2 compared to predictions based on the VGG model. Bottom: model dependent constraint on J_u and J_d obtained from a fit of this amplitude to a GPD model [13]. Please refer to Refs. [12, 14] for details.

New lattice gauge theory results [15] are consistent with these experimental findings within one sigma. Measurements from JLab Hall A on the neutron provide complementary results [16].

3 Recoil Detector at HERMES

In January 2006 the HERMES spectrometer was extended by the installation of the Recoil Detector [17], a new magnetic spectrometer surrounding the target. It consists of three detector systems:

- two layers of Silicon Strip Detectors inside the vacuum of HERA,
- two barrels of Scintillating Fibre Trackers,
- a Photon Detector of stacked lead and scintillator layers.

These are mounted inside a superconducting solenoid surrounding a storage cell target with unpolarised gases.

The main purpose of this apparatus is the measurement of the previously undetected recoiling proton from the DVCS process. The Recoil Detector is expected to reduce the background from associated BH/DVCS (intermediate Δ–production) and from semi-inclusive processes from 17% to 1%. The t resolution at small t is improved and high luminosities are achieved as unpolarised targets are used.

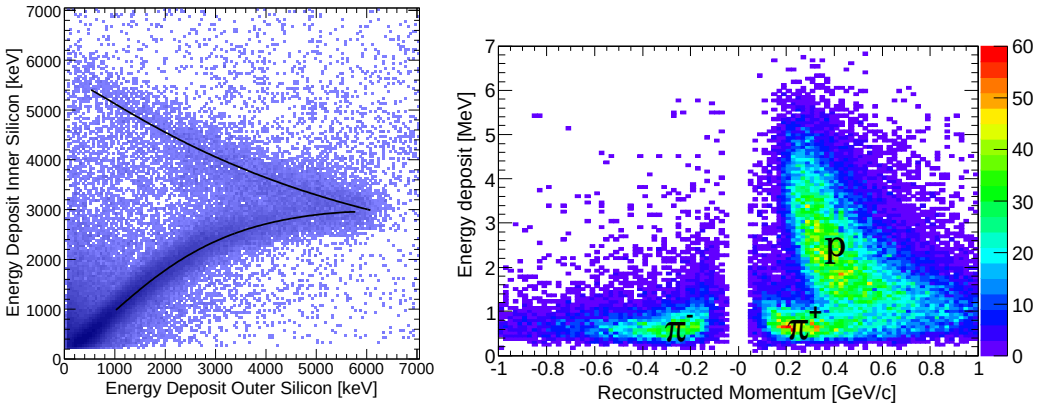

Figure 4: Left: experimental data of the energy deposited in the first and second layers of the Silicon Strip Detector. Clearly visible is the band from protons in the detectors. Also shown is the parametrisation of the expected energy deposit from Monte-Carlo studies (solid curves). Right: experimental data of energy deposited in the Scintillating Fibre Tracker versus reconstructed momentum by the curvature in the magnetic field.

The detector has been successfully commissioned in spring 2006. Data with electron and positron beams were collected, the latter data sample being

significantly larger. After first calibrations and with a preliminary momentum reconstruction in place already clean signals from protons and pions can be observed. In the left panel of Fig. 4 the band from experimental data is in good agreement with the expected energy deposit for protons obtained from Monte-Carlo studies (solid curves). From plotting the average energy losses versus the momentum reconstructed in the magnetic field of the solenoid, clear bands are observed (see right panel in Fig. 4). Thus we can clearly identify protons and pions of positive and negative charge. Currently, fine calibrations, Monte-Carlo studies and first analysis steps are being carried out.

4 Summary and Outlook

Within the framework of Generalised Parton Distributions, the measurement of hard exclusive reactions has the potential to provide access to the distributions of momentum and angular momentum of partons in the nucleon, in particular on how the spin is shared between the quarks and gluons.

The HERMES experiment has made a crucial contribution to this field already, of which only a small fraction can be presented here. Much data are still to be analysed. A large sample of data was taken in 2006 and 2007 with the new Recoil Detector, providing an almost background free exclusive data sample on Deeply Virtual Compton Scattering with improved t–resolution at small t. In particular, the large dataset will allow the Beam Spin Asymmetry to be determined more precisely. Many physics results from the HERMES collaboration can be expected to emerge in the coming years.

References

[1] A. Airapetian *et al.* [HERMES Collaboration], Phys. Rev. D **75** (2007) 012007 [Erratum-ibid. D **76** (2007) 039901].

[2] D. Mueller *et al.*, Fortsch. Phys. **42** (1994) 101.

[3] A. V. Radyushkin, Phys. Rev. D **56** (1997) 5524.

[4] X. D. Ji, Phys. Rev. Lett. **78** (1997) 610;

[5] M. Diehl *et al.*, Eur. Phys. J. C **39** (2005) 1.

[6] W. D. Nowak, Conf. Proc. St. Andrews, Scotland, Sep. 2004, [arXiv:hep-ex/0503010].

[7] K. Ackerstaff *et al.* [HERMES Collaboration], Nucl. Instrum. Meth. A **417** (1998) 230; and
K. Rith, Prog. Part. Nucl. Phys. **49** (2002) 245.

[8] A. Airapetian *et al.* [HERMES Collaboration], Phys. Rev. Lett. **87** (2001) 182001.

[9] S. Stepanyan *et al.* [CLAS Collaboration], Phys. Rev. Lett. **87** (2001) 182002.

[10] M. Vanderhaeghen, P. A. M. Guichon and M. Guidal, Phys. Rev. D **60** (1999) 094017.

[11] A. Airapetian *et al.* [HERMES Collaboration], Phys. Rev. D **75** (2007) 011103.

[12] F. Ellinghaus, W. D. Nowak, A. V. Vinnikov and Z. Ye, Eur. Phys. J. C **46**, 729 (2006).

[13] K. Goeke, M. V. Polyakov and M. Vanderhaeghen, Prog. Part. Nucl. Phys. **47** (2001) 401.

[14] Z. Ye [HERMES Collaboration], PoS **HEP2005** (2006) 120 [arXiv:hep-ex/0512010]; arXiv:hep-ex/0606061.

[15] Ph. Hagler *et al.* [LHPC Collaborations], arXiv:0705.4295 [hep-lat].

[16] M. Mazouz *et al.* [Jefferson Lab Hall A Collaboration], arXiv:0709.0450 [nucl-ex].

[17] [HERMES Collaboration], Technical Design Report, HERMES Internal Note 02-003 (2002); and
B. Seitz [HERMES Collaboration], Nucl. Instr. Meth. A **535**, 538 (2004).